0022-3565/08/3263-957–965$20.00
THE JOURNAL OF PHARMACOLOGY AND EXPERIMENTAL THERAPEUTICS
Copyright © 2008 by The American Society for Pharmacology and Experimental Therapeutics
JPET 326:957–965, 2008

Vol. 326, No. 3
138701/3372147
Printed in U.S.A.

Modulation of Sarcoplasmic Reticulum Function by PST2744 [Istaroxime; (*E*,*Z*)-3-((2-Aminoethoxy)imino) Androstane-6,17-dione Hydrochloride)] in a Pressure-Overload Heart Failure Model[S]

Marcella Rocchetti, Matteo Alemanni, Gaspare Mostacciuolo, Paolo Barassi, Claudia Altomare, Riccardo Chisci, Rosella Micheletti, Patrizia Ferrari, and Antonio Zaza

Dipartimento di Biotecnologie e Bioscienze, Università Milano-Bicocca, Milano, Italy (M.R., M.A., G.M., C.A., R.C., A.Z.); and Prassis Sigma-Tau Research Institute, Settimo Milanese, Italy (P.B., R.M., P.F.)

Received March 3, 2008; accepted June 4, 2008

ABSTRACT

PST2744 [Istaroxime; (*E*,*Z*)-3-((2-aminoethoxy)imino) androstane-6,17-dione hydrochloride)] is a novel inotropic agent that enhances sarco(endo)plasmic reticulum Ca^{2+} ATPase (SERCA) 2 activity. We investigated the istaroxime effect on Ca^{2+} handling abnormalities in myocardial hypertrophy/failure (HF). Guinea pig myocytes were studied 12 weeks after aortic banding (AoB) and compared with those of sham-operated animals (sham). The gain of calcium-induced Ca^{2+} release (CICR), sarcoplasmic reticulum (SR) Ca^{2+} content, Na^+/Ca^{2+} exchanger (NCX) function, and the rate of SR reloading after caffeine-induced depletion (SR Ca^{2+} uptake, measured during NCX blockade) were evaluated by measurement of cytosolic Ca^{2+} and membrane currents. HF characterization: AoB caused hypertrophy and failure in 100 and 25% of animals, respectively. Although CICR gain during constant pacing was preserved, SR Ca^{2+} content and SR Ca^{2+} uptake were strongly depressed. Resting Ca^{2+} and the slope of the Na^+/Ca^{2+} exchanger current (I_{NCX})/Ca^{2+} relationship were unchanged by AoB. Istaroxime effects: CICR gain, SR Ca^{2+} content, and SR Ca^{2+} uptake rate were increased by istaroxime in sham myocytes and, to a significantly larger extent, in AoB myocytes; this led to almost complete recovery of SR Ca^{2+} uptake in AoB myocytes. Istaroxime increased resting Ca^{2+} and the slope of the I_{NCX}/Ca^{2+} relationship similarly in sham and AoB myocytes. Istaroxime failed to increase SERCA activity in skeletal muscle microsomes devoid of phospholamban. Thus, clear-cut abnormalities in Ca^{2+} handling occurred in this model of hypertrophy, with mild decompensation. Istaroxime enhanced SR function more in HF myocytes than in normal ones; almost complete drug-induced recovery suggests a purely functional nature of SR dysfunction in this HF model.

Positive inotropic interventions remain essential in the management of heart failure; nonetheless, their use is strongly limited by proarrhythmic effects and increased oxygen consumption. We have shown that, in normal myocytes, the positive inotropic effect of Na^+/K^+ pump inhibition can be dissociated from proarrhythmia if SERCA2 is stimulated (Rocchetti et al., 2005). The two actions are simultaneously exerted by the compound PST2744 (istaroxime), whose therapeutic index (inotropy/proarrhythmia) largely exceeds the one of digoxin in single-cell and whole-animal studies (Micheletti et al., 2002; Rocchetti et al., 2003). The favorable therapeutic profile of istaroxime has been confirmed in animal models of heart failure (Mattera et al., 2007; Sabbah et al., 2007) and in man (Ghali et al., 2007). However, whether

This study was supported by the Istituto di Ricerche Prassis Sigma-Tau and by FAR Università Milano-Bicocca to A.Z.

Parts of this work were presented in abstract form as follows: Rocchetti M, Alemanni M, Micheletti R, Ferrari P, and Zaza A (2007) Istaroxime modulation of sarcoplasmic reticulum function in cardiac hypertrophy/failure. In Winter Meeting on Translational Basic Science of the Heart Failure Association; 2007 Jan 24–27; Garmisch-Parten Kirchen, Germany.

Article, publication date, and citation information can be found at http://jpet.aspetjournals.org.

doi:10.1124/jpet.108.138701.

[S] The online version of this article (available at http://jpet.aspetjournals.org) contains supplemental material.

ABBREVIATIONS: SERCA, sarco(endo)plasmic reticulum Ca^{2+} ATPase; PST2744, (*E*,*Z*)-3-((2-aminoethoxy)imino) androstane-6,17-dione hydrochloride); SR, sarcoplasmic reticulum; PLB, phospholamban; AoB, aortic banding; HW/BW, heart weight/body weight ratio; LW/BW, lung weight/body weight ratio; C_m, membrane electrical capacity; I_{CaL}, L-type Ca^{2+} current; I_{NCX}, Na^+/Ca^{2+} exchanger current; CICR, Ca^{2+}-induced Ca^{2+} release; Ca_f, free cytosolic Ca^{2+} concentration; NCX, Na^+/Ca^{2+} exchanger; Ca_{SRT}, total sarcoplasmic reticulum Ca^{2+} content; Ca_{rest}, resting Ca^{2+} at −80 mV; τ_{decay}, time constant of Ca^{2+} transient relaxation; dCa/dt_{max}, maximum velocity of Ca^{2+} rise; ANOVA, analysis of variance; CV, coefficient(s) of variation; RyR, ryanodine receptor; I_m, membrane current; a.u., arbitrary unit(s); Lcyt, liters of cytosol.

this can still be attributed to SERCA2 stimulation is an open question.

Dysfunction of the sarcoplasmic reticulum (SR) is a key feature in myocardial remodeling and is considered as a central mechanism in a wide spectrum of hypertrophy/failure etiologies. Such functional impairment has been variably attributed to down-regulation of SERCA2 protein transcription and/or to an increase in the inhibitory (unphosphorylated) form of phospholamban (PLB) (Bers, 2006). Thus, the expression and conformation of the molecular target of istaroxime may be changed in the failing myocardium, with unknown consequences on its effect. At a more general level, the question is how molecular remodeling may affect the response of drugs acting through SERCA2 modulation.

The present study aims to test whether istaroxime is capable of stimulating SR Ca^{2+} uptake also in the presence of cardiac hypertrophy/failure. To this end, modulation of Ca^{2+} handling by istaroxime was tested in an experimental model of cardiac dysfunction in which chronic pressure overload was induced by aortic constriction in the guinea pig. The results obtained show that SR impairment can be largely reversed by pharmacological means in this model. This leads to a "functional" interpretation of SERCA2 abnormality, potentially relevant to the therapy of contractile dysfunction. Such an interpretation suggests that istaroxime may act by preventing the interaction between SERCA and PLB. To obtain a preliminary evaluation of this hypothesis, we also tested istaroxime effect on SERCA activity in skeletal muscle microsomes devoid of PLB. This collateral observation is reported in the supplemental data.

Materials and Methods

The investigation conforms to the *Guide for the Care and Use of Laboratory Animals* published by the Institute of Laboratory Animal Resources (1996) and to the guidelines for animal care endorsed by the hosting institution.

Aortic Banding Model

Chronic pressure overload was induced in guinea pigs after banding of the ascending aorta (AoB) under ketamine (100 mg/kg)-xylazine (5 mg/kg) i.p. Sham-operated littermates (sham) were used as controls.

Myocyte Preparation and Recording Solutions

Guinea pigs were killed by cervical dislocation under ketamine-xylazine anesthesia 12 weeks after AoB. Cardiac hypertrophy/heart failure was evaluated through the heart weight/body weight (HW/BW) and lung weight/body weight (LW/BW) ratios. Ventricular myocytes were isolated by using a retrograde coronary perfusion method previously published (Zaza et al., 1998), with minor modifications. Rod-shaped, Ca^{2+}-tolerant myocytes were used within 12 h from dissociation.

During measurements, myocytes were superfused at 2 ml/min with Tyrode's solution containing 154 mM NaCl, 4 mM KCl, 2 mM $CaCl_2$, 1 mM $MgCl_2$, 5 mM HEPES-NaOH, and 5.5 mM D-glucose, adjusted to pH 7.35. The pipette solution contained 110 mM K^+-aspartate, 23 mM KCl, 0.2 mM $CaCl_2$ (calculated free $Ca^{2+} = 10^{-7}$ M), 3 mM $MgCl_2$, 5 mM HEPES KOH, 0.5 mM EGTA KOH, 0.4 mM GTP-Na salt, 5 mM ATP-Na salt, and 5 mM creatine phosphate Na salt, pH 7.3. Tyrode and pipette solutions were modified for the SR reloading protocol, as detailed in *Experimental Protocols* (below). A thermostated manifold, allowing for a fast (electronically timed) solution switch, was used for cell superfusion. All measurements were performed at 35 ± 0.5°C. Throughout the present study, istaroxime was tested at the concentration of 4 μM, corresponding to the steep portion of the concentration-response curve for inotropy (Micheletti et al., 2002) and shown to be effective on SR function of normal myocytes of the same species (Rocchetti et al., 2005).

Electrophysiology Techniques

Ventricular myocytes were voltage-clamped in the whole-cell configuration (Axopatch 200-A; Molecular Devices, Sunnyvale, CA). Membrane capacitance (C_m) and series resistance were measured in every cell but left uncompensated; the average values of series resistance in sham and AoB experiments were 5.1 ± 0.2 (n = 48) and 5.0 ± 0.2 (n = 63) (N.S.) MΩ, respectively. Current signals were filtered at 2 kHz and digitized at 5 kHz (Axon Digidata 1200). Trace acquisition and analysis was controlled by dedicated software (Axon pClamp 8.0). Guinea pig ventricular myocytes do not express I_{to} (Zicha et al., 2003); thus, peak inward current measured upon depolarizations from a holding potential of −40 mV (I_{Na} fully inactivated) essentially reflects Ca^{2+} influx through I_{CaL} and Na^+/Ca^{2+} exchanger current (I_{NCX}); this was confirmed in preliminary experiments (see Supplemental Fig. 1). It is fair to stress that inward current, albeit adequate to calculate Ca^{2+}-induced Ca^{2+} release (CICR) gain (see below), cannot be assumed to reflect I_{CaL}. Accurate measurement of I_{CaL} requires series resistance compensation, estimation of time-dependent run-down, and intracellular K^+ substitution by Cs^+, none of which was implemented in the present experiments. In particular, K^+ substitution by Cs^+ was avoided because it affects SR function (Kawai et al., 1998), the main object of this study.

Measurements of Intracellular Ca^{2+}

Single-myocyte intracellular Ca^{2+} activity was measured fluorometrically using the membrane-permeable dye Indo1-AM (8 μM; Invitrogen, Carlsbad, CA) as described previously. Indo1-AM fluorescent emission was measured at two wavelengths (410 and 490 nm) (Grynkiewicz et al., 1985). The signals at the two wavelengths (F_{410} and F_{490}) were separately low-pass filtered (200 Hz) and digitized at 2 kHz. Cytosolic Ca^{2+} activity was calculated from the F_{410}/F_{490} ratio after low-pass digital filtering (FFT, 100 Hz) and subtraction of the background luminescence. Conversion of F_{410}/F_{490} ratio to free cytosolic Ca^{2+} concentration (Ca_f) was performed as described by Sipido and Callewaert (1995) after dye calibration in ionomycin permeabilized myocytes (Rocchetti et al., 2005).

Measurement of SERCA Activity in SR Microsomes

The methods for this set of experiments are reported in the supplemental data, where the relevant results are also presented.

Experimental Protocols

Protocol 1 (Caffeine Pulse Protocol). Transmembrane current (holding potential −80 mV) and cytosolic Ca^{2+} were simultaneously recorded (in Tyrode's solution) during a 5-s caffeine pulse (10 mM) applied 10 s after a loading train of voltage steps (−40 to 0 mV, 200 ms, 0.37 Hz).

Protocol 2 (SR Reloading Protocol). The Na^+/Ca^{2+} exchanger (NCX) was inhibited by 30-min cell incubation in an Na^+- and Ca^{2+}-free solution (replaced by equimolar Li^+ and 1 mM EGTA). SR was initially depleted by a brief caffeine pulse (with 154 mM Na^+ to allow Ca^{2+} extrusion through the NCX) and then progressively reloaded by a train of depolarizing pulses (−40 to 0 mV, 200 ms, 0.25 Hz) in the presence of 1 mM Ca^2. The pipette solution was Na^+-free (Na^+ salts were replaced by K^+ or Tris salts).

Estimation of Functional Parameters

Total SR Ca^{2+} content (Ca_{SRT}; in micromoles per liter of cytosolic volume) was estimated by integrating the I_{NCX} elicited by the caffeine pulse (protocol 1) and dividing the nanomoles of Ca^{2+} by the estimated cell volume (C_m/6.44) (Bers, 2002d) (Table 1). I_{NCX} was defined as the transient component of caffeine-induced membrane

TABLE 1
Glossary of symbols and method of calculation

Symbol	Meaning	Formula	Parameters	References
Ca_f	Free cyt. Ca^{2+} (molar concentration)	$K_d \times \beta \times \frac{R - R_{min}}{R_{max} \times R}$	K_d = 250 nM; R_{min} = 0.24; R_{max} = 0.86; β = 2.54	(Grynkiewicz et al, 1985); from dye calibration
Ca_{NCX}	Ca^{2+} through I_{NCX} (moles)	$1/zF \times \int dI_m \times dt$	z = 1; F = Faraday constant	Bers, 2002a
Ca_{SRT}	SR Ca^{2+} content (moles/Lcyt.)	$\frac{Ca_{NCX}}{V_{cyt}}$	Ca_{NCX} from caffeine pulse; $V_{cyt} = C_m/6.44$	Bers, 2002a

cyt., cytosol; I_m, membrane current; K_d, dissociation constants; R_{min}, R_{max}, and β, indo-1 calibration parameters (Grynkiewicz et al, 1985); V_{cyt}, volume of cytosol.

current; thus, the steady-state current present during caffeine superfusion (pedestal) was subtracted before integration.

The NCX function was evaluated by plotting I_{NCX} as a function of Ca_f during caffeine pulses (protocol 1). The slope of this relation was obtained by linear interpolation of the points in the final third of Ca^{2+} transient relaxation, when bulk cytosolic Ca_f values more closely reflect subsarcolemmal ones (Bers, 2002c) (cells in which the I_{NCX}/Ca_f relation was entirely nonlinear were not used for this analysis). The steady-state value of Ca_f measured at holding potential just before caffeine application will be referred to as "resting" Ca^{2+} (Ca_{rest}).

The Ca^{2+} uptake function of SR (SERCA2 uptake flux minus leak flux) was dynamically tested by the SR reloading protocol (protocol 2). The rate of SR reloading was determined from the increment of Ca^{2+} transient amplitude in subsequent voltage steps delivered after caffeine-induced depletion. The time constant of Ca^{2+} transient relaxation (τ_{decay}), reflecting the rate of net SR Ca^{2+} uptake, was measured during each step of the reloading process by monoexponential fit of the Ca^{2+} transient decay. In consideration of the dependence of SERCA2 activity from cytosolic Ca^{2+} (Bers and Berlin, 1995), τ_{decay} was also plotted as a function of peak Ca_f achieved during each step (see Supplemental Fig. 2).

The amplification factor in CICR gain was calculated according to two methods. In the first one, peak amplitude of Ca^{2+} transient was divided by "peak inward current"; in the second one, the maximum velocity of Ca^{2+} rise (dCa/dt_{max}) was divided by peak inward current. Both methods use peak inward current in lieu of Ca^{2+} influx, thus yielding a value in arbitrary units (Bers, 2002b). This approach was preferred because an absolute estimate of CICR gain was beyond the aims of this study, and the peak value of inward current may more accurately reflect Ca^{2+} influx under the present experimental conditions. It should be stressed that, because Ca^{2+} release and Ca^{2+} influx are linearly related (Bers, 2002b), their ratio is independent of their absolute value.

Substances

Stock Indo1-AM solution (1 mM in dry dimethyl sulfoxide) was diluted in Tyrode's solution. Istaroxime was dissolved in water. Istaroxime (PST2744; chemical structure in Micheletti et al., 2002; Rocchetti et al., 2003) was synthesized at Prassis Sigma-Tau (Settimo Milanese, Italy), Indo-1AM was from Molecular Probes, and all other chemicals were obtained from Sigma-Aldrich (St. Louis, MO).

Statistical Analysis

Sham and AoB conditions are represented by distinct experimental groups; to minimize the effect of intersubject variability, data were collected from more than five animals in each condition. Sham and AoB animals were studied in alternate sequence. Individual means were compared by paired or unpaired Student's t test as appropriate; in the SR loading protocol, differences were tested by two-way ANOVA, applied to either absolute values or istaroxime-induced changes. Statistical significance was defined as $p < 0.05$ (N.S., not significant). The least-square method was used for linear and nonlinear fitting and parameter estimation. Data are expressed as mean ± S.E. of independent determinations; the coefficient of variation (CV) was calculated as the ratio between S.D. and mean. Sample size (number of cells) is specified for each experimental condition in the tables and figure legends.

Results

The evaluations included in this study required the development and characterization of a model of aortic banding in the guinea pig, whose effects have not been described previously. In this section, the observations concerning the functional characterization of the model will be reported first and will be followed by the description of istaroxime effects in sham and AoB animal groups. Results concerning the effect of istaroxime on SERCA activity in microsomes are reported in the supplemental data.

Functional Characterization of the AoB Model. This section of results compares myocardial function of animals 12 weeks after AoB with that of sham of the same gender. HW/BW, LW/BW, and C_m of shams and AoB animals are compared in Table 2. HW/BW was significantly increased by AoB. There was a tendency to increase the LW/BW ratio in AoB. Because of the large scatter, this change did not achieve statistical significance; however, in 25% of AoB animals, the LW/BW ratio was more than 2-fold the average of sham animals. C_m was significantly larger after AoB to indicate an increase in cell size. Within the study period, mortality was null in both sham and AoB groups. As shown in Fig. 1, Ca_{SRT} was decreased by approximately 32% after AoB ($p < 0.05$ versus sham) (Fig. 1B).

During the SR reloading protocol, the parameters of Ca^{2+} transients (amplitude and τ_{decay}) and the CICR gain changed over subsequent depolarizing pulses (Fig. 2), reflecting a progressive increase in the SR Ca^{2+} content. Thus, the analysis of the time course of these parameters provides information on the SR Ca^{2+} uptake function (Rocchetti et al., 2005). After AoB, the time courses of Ca^{2+} transient amplitude and

TABLE 2
AoB model parameters

	HW/BW	CV	LW/BW	CV	C_m	CV
	g/kg		*g/kg*		*pF*	
Sham (N = 8)	4.37 ± 0.24	0.16	5.24 ± 0.32	0.17	216 ± 14 (n = 48)	0.46
AoB (N = 12)	6.56 ± 0.50*	0.25	5.95 ± 0.82	0.50	303 ± 14 (n = 63)*	0.38

* $P < 0.05$ vs. sham animals; N = no. of animals; n = no. of cells.

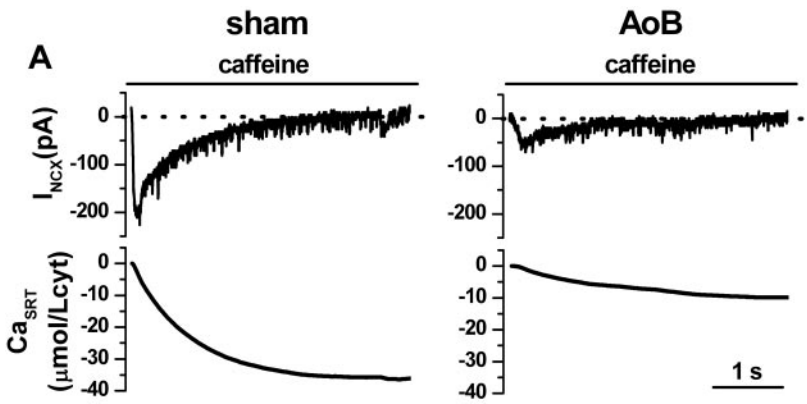

Fig. 1. AoB effect on Ca_{SRT}. A, representative examples of caffeine-induced I_{NCX} (holding potential, −80 mV) and the corresponding cumulative I_{NCX} integrals in a sham (left) and AoB (right) myocyte. B, average results of Ca_{SRT} (for method, see Table 1), in sham (n = 30) and AoB (n = 28) myocytes; *, $p < 0.05$ versus sham.

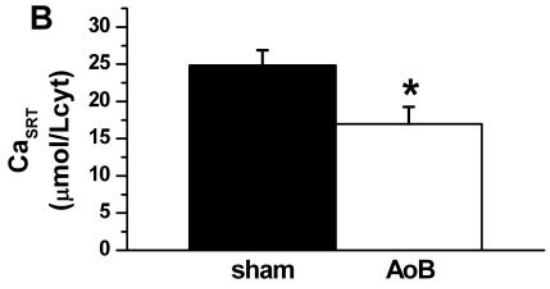

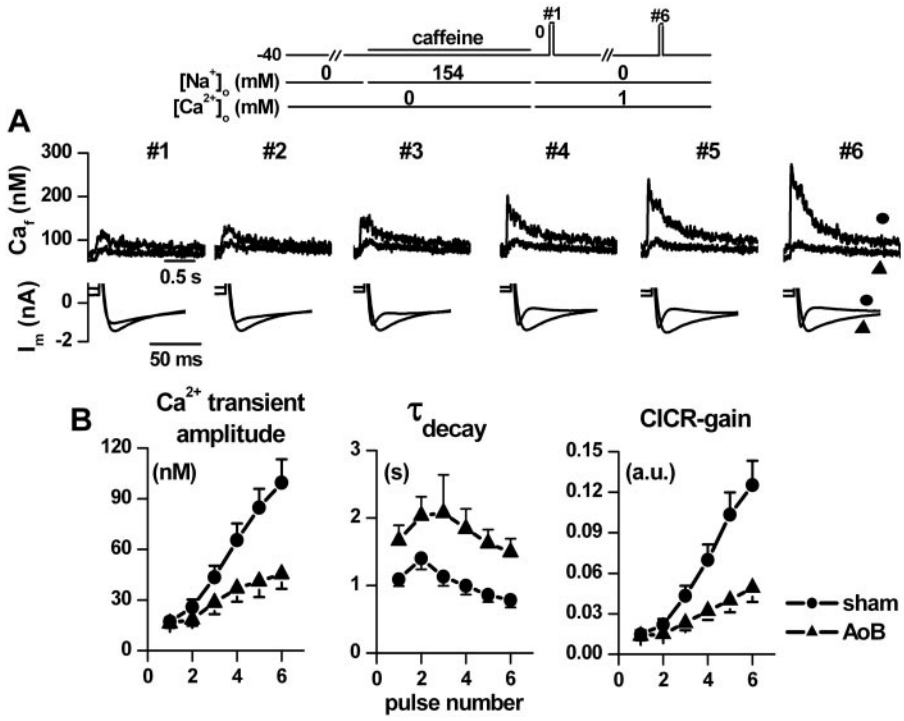

Fig. 2. AoB effect on SR function (with blocked NCX). A, example of Ca_f and membrane current (I_m) recorded during SR reloading after caffeine-induced SR depletion in sham (●) and AoB (▲) myocytes; recordings were performed in the absence of NCX function (Na^+-free Tyrode and pipette solutions). B, average values of Ca^{2+} transient parameters measured during each pulse (1–6) of the stimulation train in sham (●, n = 23) and AoB (▲, n = 22) myocytes. CICR gain (measured as the ratio between the Ca^{2+} transient amplitude and the peak inward current) was expressed in arbitrary units (a.u.) (see *Materials and Methods*). Inset, outline of the experimental protocol. Significance of AoB-induced changes was detected by two-way ANOVA ($p < 0.05$ for all variables).

CICR gain were markedly slowed compared with sham animals; τ_{decay} was uniformly increased over the whole reloading train (Fig. 2B). Differences between sham and AoB myocytes in the time course of all variables were significant ($p < 0.05$), as tested by two-way ANOVA. The change in τ_{decay} was evident also when compared at similar cytosolic Ca^{2+} concentrations (measured at the beginning of the decay of Ca^{2+} transient; see Supplemental Fig. 2). The changes in Ca^{2+} transient amplitude occurring during the loading protocol and between sham and AoB myocytes (Fig. 2A) are accompanied by changes in amplitude and inactivation rate of inward current, as expected from Ca^{2+}-dependent inactivation of I_{CaL} (Lee et al., 1985).

In contrast to the marked depression of SR function detected by the reloading protocol (protocol 2), during steady-state stimulation in normal Tyrode (protocol 1) the amplitudes of V-induced Ca^{2+} transients (111.2 ± 11 versus 106.8 ± 9 nM, N.S.), their dCa/dt_{max} (12.7 ± 1.3 versus 13.0 ± 1.0 nM/ms, N.S.), and peak inward current (−4.44 ± 0.32 versus −3.99 ± 0.36 nA, N.S.) were similar between

sham and AoB myocytes. Accordingly, CICR gain was unchanged between the two conditions, independently of the method used for its evaluation (Fig. 3). The slope of the I_{NCX}/Ca_f relation and Ca_{rest} were unchanged by AoB (Fig. 4).

Istaroxime Effects in Sham versus AoB Groups. Istaroxime (4 μM) was acutely applied to myocytes from sham and AoB groups, and evaluation of functional parameters was performed as above. In sham myocytes, istaroxime effects were similar to those previously reported for normal guinea pig myocytes (Rocchetti et al., 2005; Micheletti et al., 2007). Istaroxime increased SR Ca^{2+} content by 79.2 ± 21.1% ($p < 0.05$ versus control; Fig. 5). Stimulation of SR Ca^{2+} uptake function by istaroxime was also evident during the SR reloading protocol, in which NCX contribution was absent (see *Materials and Methods*, protocol 2). The rate of change of Ca^{2+} transient amplitude and CICR gain during the reloading process was increased, and τ_{decay} was shortened by the drug (Fig. 6). Differences between baseline and istaroxime superfusion in the time course of all variables were significant ($p < 0.05$), as tested by two-way ANOVA. Consistently with stimulation of SR uptake function, istaroxime increased CICR gain measured under normal Tyrode superfusion (functioning NCX; Fig. 7); istaroxime also increased the slope of the I_{NCX}/Ca_f relationship by 93.3 ± 35% ($p < 0.05$ versus control; Fig. 8) and Ca_{rest} by 41.3 ± 9.9% ($p < 0.05$ versus control; Fig. 8).

After AoB, istaroxime increased Ca_{SRT} by an average of 136.9 ± 31.9% ($p < 0.05$); although apparently larger, this effect was not significantly different from that observed in sham myocytes (79.2 ± 21.1%; N.S. versus AoB). Figure 5C shows that failure to achieve significance was because of a wide scatter in istaroxime effect among cells. Rather than being casually variable, istaroxime effect was inversely related to the Ca_{SRT} level measured in control condition to steeply increase for values below 20 μmol/Lcyt. Stimulation of SR Ca^{2+} uptake by istaroxime was fully preserved in AoB myocytes, in which baseline SR function was depressed (Fig. 6B). Istaroxime effect on the increase in Ca^{2+} transient amplitude during the reloading protocol was actually larger in AoB than in sham myocytes (two-way ANOVA, $p < 0.05$). For the other parameters (τ_{decay} and CICR gain), istaroxime effect, although highly significant in both groups, was not significantly different between sham and AoB myocytes, probably because of the larger scatter of values. The absolute SR performance achieved under istaroxime in AoB myocytes approached that observed in sham myocytes (Fig. 6B) to indicate substantial recovery of AoB-induced dysfunction.

CICR gain (measured by protocol 1) was similarly increased by istaroxime in AoB and sham myocytes (Fig. 7). The slope of I_{NCX}/Ca_f relationship (+173 ± 89%) and Ca_{rest} (+29 ± 5%) were also increased by istaroxime; the effect was again similar between sham and AoB myocytes (Fig. 8).

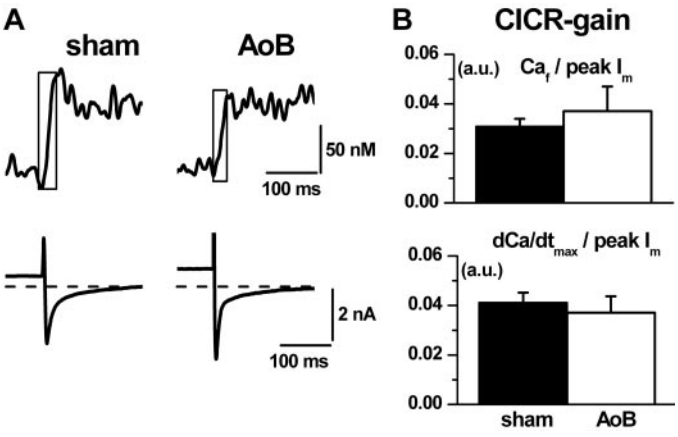

Fig. 3. AoB effect on CICR gain. A, Ca_f and I_m simultaneously recorded during voltage steps (from −40 to 0 mV for 200 ms) in a sham (left) and AoB (right) myocyte. B, average values of CICR gain (calculated according to two methods and expressed in a.u., see *Materials and Methods*) in sham ($n = 33$) and AoB ($n = 27$) myocytes; dCa/dt_{max} was calculated during the rising phase of the Ca^{2+} transient (boxes in A).

Discussion

Features of the AoB Model. The pressure overload model used in the present study has been previously characterized in vivo at 12 weeks after banding of the ascending aorta, with findings compatible with left ventricular hypertrophy and mild failure (Micheletti et al., 2007); the present ex vivo observations (Table 2) are substantially in agreement with in vivo ones. HW/BW and C_m were consistently increased after AoB, thus reflecting clear-cut myocardial hypertrophy in all cases. Lung congestion was present in a minority of cases. The absence of mortality in the AoB groups rules out the possibility that the hearts used for cell studies may come from a surviving subpopulation, i.e., one with particularly mild abnormalities. Cardiac decompensation observed in the present work was mild compared with that observed in guinea pigs studied up to 8 weeks after banding of descending aorta (Kiss et al., 1995; Ahmmed et al., 2000).

The main functional derangement observed in myocytes from AoB animals concerned SR Ca^{2+} uptake function. This was manifested by a marked depression of SR reloading (after caffeine-induced depletion) (Fig. 2). In contrast, reduction in SR Ca^{2+} content was relatively milder (−32%; Fig. 1), and CICR gain during steady-state stimulation under normal Tyrode superfusion was unchanged (Fig. 3). Considering that SR reloading was measured starting from very low cell Ca^{2+} content and during NCX blockade, the discrepancy might suggest that the derangement in SR uptake function may be unveiled by low Ca^{2+} content and partially compensated by NCX function. The observation that the reduction of SR Ca^{2+} content was not associated with a decrease in CICR gain might suggest that the ryanodine receptor (RyR) sensitivity to cytosolic Ca^{2+} was increased in AoB myocytes, as commonly observed in the failing heart (Yano et al., 2005).

Abnormalities of the SR uptake function, as those detected in this study, can be due to reduced SERCA2 activity or to increased Ca^{2+} leak through RyR channels. Previous biochemical evaluations showed that maximal ATPase activity of SERCA2 is decreased in this model, despite normal expression of SERCA2 protein (Micheletti et al., 2007). Reduced SERCA2 activity might result from an increase in the unphosphorylated (monomeric) form of PLB, previously described in this model (Micheletti et al., 2007). In this case, SERCA2 abnormality would be functional, rather than structural, a view also supported by the effect of istaroxime discussed below. This pattern differs from that more often described in hypertrophy, in which a decrease in SERCA2 expression contributes to down-regulation of SR Ca^{2+} transport (Bers, 2006).

Ca^{2+} dependence of I_{NCX} was unchanged after AoB (Fig.

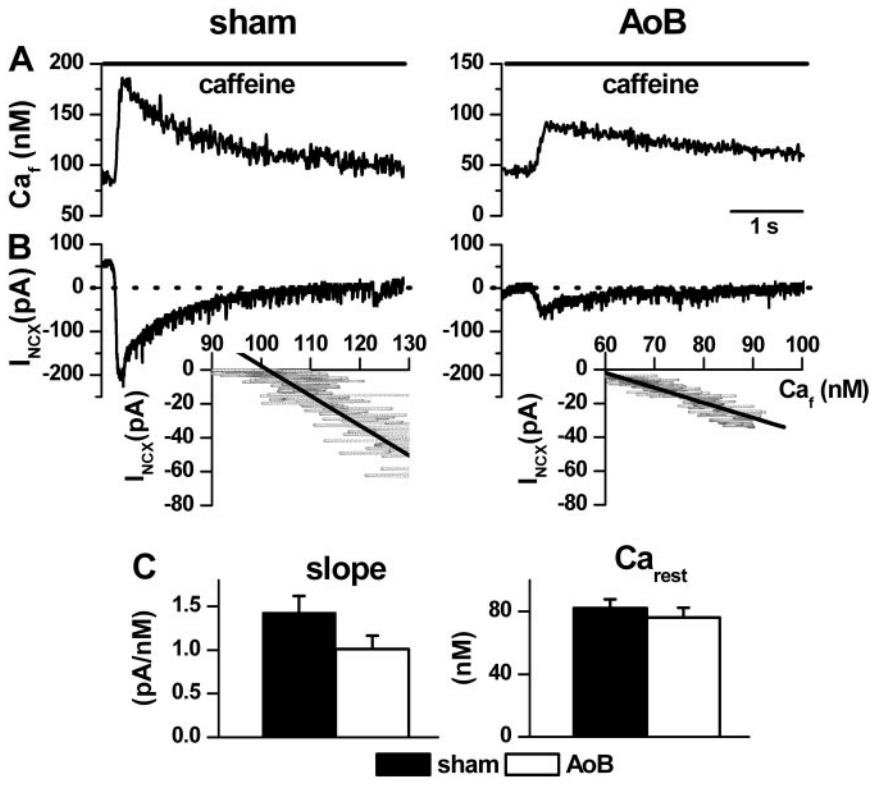

Fig. 4. AoB effect on NCX function. A and B, Ca_f and the I_{NCX} simultaneously recorded during caffeine superfusion (holding potential, −80 mV) in a sham (left) and AoB (right) myocyte; I_{NCX}/Ca_f relationships and their linear interpolation (solid lines) in the final third of Ca^{2+} transient relaxation are shown in the insets. C, average results of the slope of the I_{NCX}/Ca_f relationship and resting Ca^{2+} measured at −80 mV (Ca_{rest}) in sham (n = 24) and AoB (n = 24) myocytes.

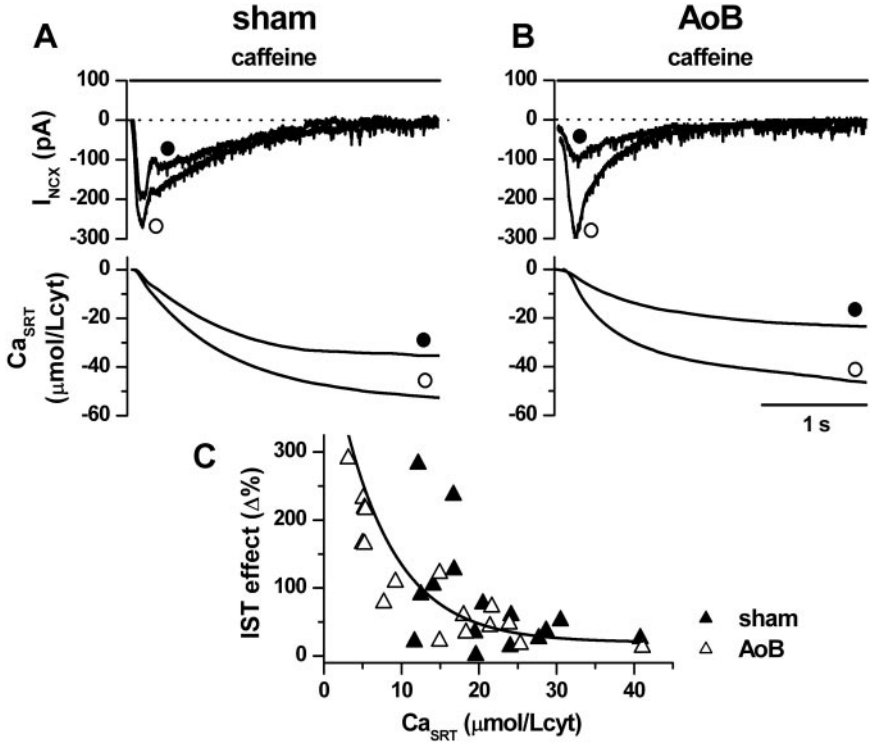

Fig. 5. Istaroxime effects in sham versus AoB groups: effect on Ca_{SRT}. A and B, representative examples istaroxime (IST, 4 μM; ○) effect on the caffeine-induced I_{NCX} (holding potential, −80 mV) and the corresponding cumulative I_{NCX} integrals in a sham and AoB myocyte. C, IST effect (Δ% increase of Ca_{SRT}) as a function of Ca_{SRT} level measured in control (cont, ●) in all experimental conditions [data groups from sham (▲, n = 15) and AoB (△, n = 18); groups were pooled together]; continuous line represents the best exponential fit of the experimental data.

4). This finding is apparently at variance with up-regulation of NCX protein expression and enhancement of I_{NCX} reported in human heart failure (Studer et al., 1994; Pieske et al., 1999) and in hypertrophy models in various species, including guinea pig (Ahmmed et al., 2000). Although NCX protein expression was not evaluated in the present work, the functional observations are not necessarily in contrast with previous ones in the same species. In the work on guinea pig by Ahmmed et al. (2000), I_{NCX} was measured upon repolarization after long depolarizing steps (tail current). An increase in I_{NCX} tail current can be because of either genuine up-regulation of NCX function or simply because of an increase in cytosolic Ca^{2+} levels achieved during the depolarizing step (Barcenas-Ruiz et al., 1987). Under the conditions of the

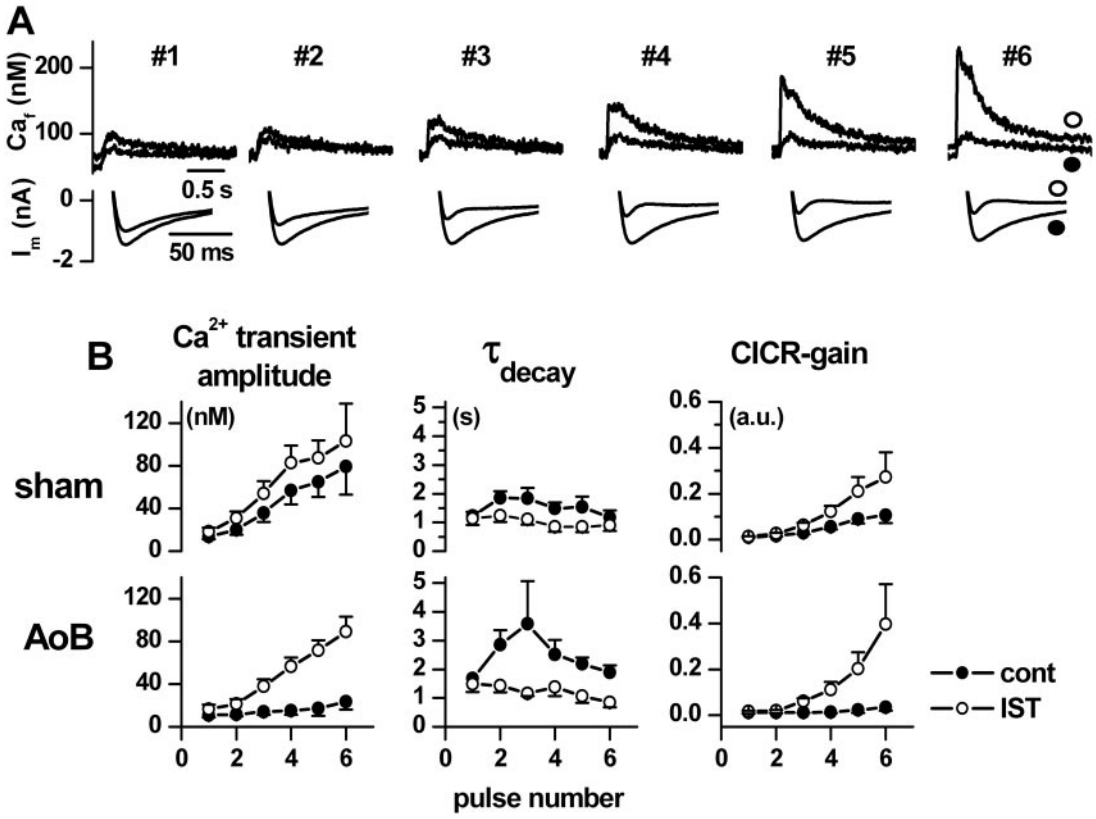

Fig. 6. Istaroxime effects in sham versus AoB groups: effect on SR function with blocked NCX. A, example of Ca_f and I_m recorded in an AoB myocyte during SR reloading after caffeine-induced SR depletion in control (cont, ●) and after istaroxime superfusion (IST, 4 μM; ○); recordings were performed in the absence of NCX function (Na^+-free Tyrode and pipette solutions); the protocol is outlined in Fig. 2. B, average values of Ca^{2+} transient parameters measured during each of the first six pulses (1–6) of the stimulation train in cont (●) and after IST superfusion (○), in sham ($n = 11$) and AoB ($n = 8$) myocytes. The decay time constant (τ_{decay}) was estimated by a monoexponential fit of the Ca^{2+} transient decay; CICR gain (measured as the ratio between the Ca^{2+} transient amplitude and the peak inward current) was expressed in a.u. Significance of istaroxime effects was tested by two-way ANOVA on all variables for both sham and AoB groups (see text).

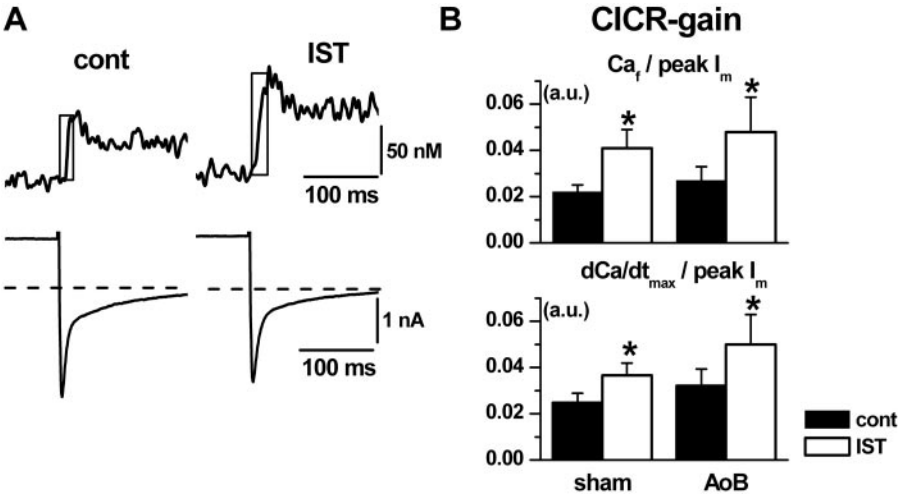

Fig. 7. Istaroxime effects in sham versus AoB groups: effect on CICR gain. A, Ca_f and I_m simultaneously recorded during voltage steps (from −40 to 0 mV for 200 ms) in a sham myocyte, in control (cont) and after istaroxime superfusion (IST 4 μM). B, average values of CICR gain (calculated according to two methods and expressed in a.u.; see *Materials and Methods*) in control and after IST superfusion in sham ($n = 13$) and AoB ($n = 17$) myocytes; dCa/dt_{max} was calculated during the rising phase of the Ca^{2+} transient (boxes in A). *, $p < 0.05$ versus cont.

study by Ahmmed et al. (CICR suppression), the latter may be justified in hypertrophied myocytes by depressed SR Ca^{2+} uptake. In the present experiments, NCX function was defined through the relationship between I_{NCX} and cytosolic Ca^{2+}, thus correcting for differences in cytosolic Ca^{2+} level. Nevertheless, in species other than guinea pigs, the same analysis detected an increase of NCX function in hypertrophy (Díaz et al., 2004); thus, it is difficult to rule out that differences in NCX function between this and previous studies may be real and possibly related to the severity of hemodynamic overload.

Istaroxime Effects in Sham and AoB Myocytes. In myocytes from sham-operated animals istaroxime improved Ca^{2+} handling, as previously reported in normal hearts of the same species (Rocchetti et al., 2005). Under ionic conditions in which all Ca^{2+} handling mechanisms were operative (normal Tyrode), istaroxime increased total SR Ca^{2+} content (Fig. 5), which implies a shift of the balance between Ca^{2+}

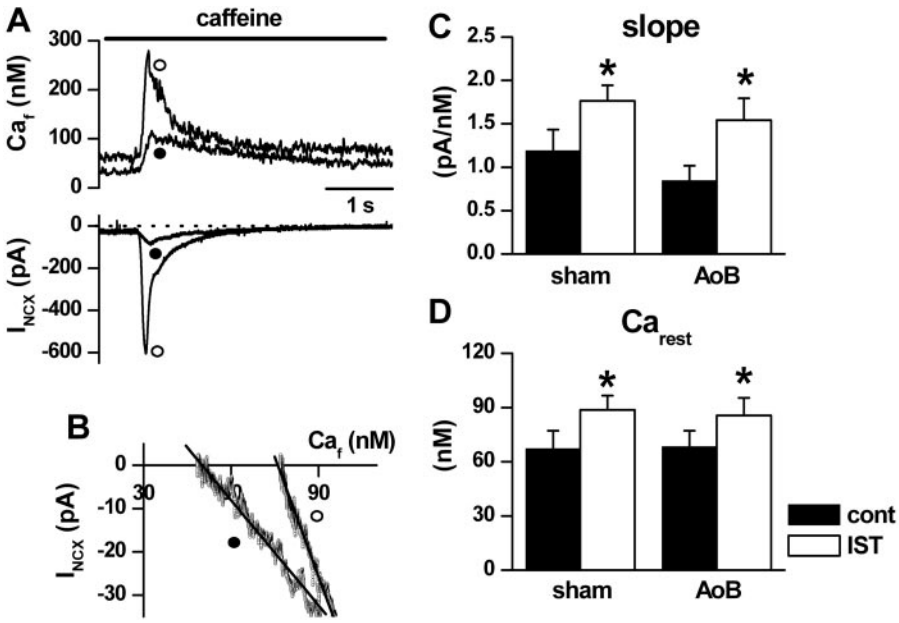

Fig. 8. Istaroxime effects in sham versus AoB groups: effect on NCX function. A, Ca_f and the I_{NCX} simultaneously recorded in a sham myocyte during caffeine superfusion (holding potential, −80 mV) in control (cont, ●) and after istaroxime superfusion (IST, 4 μM; ○); Ca_f and I_{NCX} traces recorded in cont and IST were time aligned for clarity; I_{NCX} traces were also offset to 0 level at the end of caffeine pulse. B, I_{NCX}/Ca_f relationships and their linear interpolation (solid lines) in the final third of Ca^{2+} transient relaxation. C and D, average results of the slope of the I_{NCX}/Ca_f relationship and resting Ca^{2+} measured at −80 mV (Ca_{rest}) in cont and after IST superfusion in sham ($n = 8$) and AoB ($n = 11$) myocytes; *, $p < 0.05$ versus cont.

uptake by SR and Ca^{2+} extrusion from the cell. In turn, SR Ca^{2+} uptake rate reflects the balance between active Ca^{2+} transport (by SERCA2) and passive Ca^{2+} leak through RyR channels, both fluxes being enhanced by high cytosolic Ca^{2+} (Meissner and Henderson, 1987; Shannon et al., 2000). As shown by previous studies in intact myocytes and isolated SR vesicles, istaroxime actions include inhibition of the Na^+/K^+ pump and stimulation of SERCA2 ATPase activity (Rocchetti et al., 2003, 2005) (also see the supplemental data). Although both these actions may concur to increase SR Ca^{2+} content, the former depends on the change in NCX electrochemical equilibrium, secondary to elevation of cytosolic Na^+. When tested under conditions of complete inhibition of NCX function (Na^+-free conditions), istaroxime was still able to stimulate SR Ca^{2+} uptake, as reflected by an increase in the rate at which SR reloads after depletion and by an acceleration of Ca^{2+} decay after voltage-induced transients (Fig. 6). These observations suggest that istaroxime-induced increase in SR Ca^{2+} content may also occur through SERCA2 stimulation, i.e., independently of Na^+/K^+ pump inhibition. Istaroxime also increased the efficacy by which Ca^{2+} influx triggers SR Ca^{2+} release (CICR gain) (Fig. 7), probably an effect secondary to the increase in luminal SR Ca^{2+} (Xu and Meissner, 1998; Rocchetti et al., 2005). Istaroxime increased both the *x*-axis intercept (Ca_f at $I_{NCX} = 0$) and the slope of the I_{NCX}/Ca_f relationship (Fig. 8). The intercept change may result from an increase in cytosolic Na^+ and was expected from istaroxime effect on the Na^+/K^+ pump (Rocchetti et al., 2003). According to previous evidence, istaroxime does not directly stimulate NCX (Rocchetti et al., 2003); thus, the increase in the slope of the I_{NCX}/Ca_f relationship is more likely because of allosteric modulation of the exchanger by elevated Ca_f (Weber et al., 2001). The net effect of these two changes is a reduction in the rate of Ca^{2+} extrusion through NCX at resting membrane potential (−80 mV).

The rather severe SR dysfunction observed after AoB was almost completely reversed by istaroxime (Figs. 5 and 6). This implies that the dysfunction was exclusively functional and is consistent with the lack of SERCA2 protein downregulation in this model (Micheletti et al., 2007).

Istaroxime Effect in Skeletal versus Cardiac SR Microsomes. The ability of istaroxime to recover the SR abnormality in AoB myocytes suggests that this agent may interfere with SERCA modulation by PLB. This is also consistent with the finding that istaroxime stimulates SERCA2 in cardiac microsomes from healthy guinea pig by increasing its affinity for cytosolic Ca^{2+} (Rocchetti et al., 2005; Micheletti et al., 2007) (see also supplemental data and Supplemental Fig. 4), which is limited by the interaction with PLB (Waggoner et al., 2007).

The observation reported in the supplemental data that istaroxime was unable to increase SERCA activity in skeletal muscle microsomes, which are naturally devoid of PLB, provides a preliminary support to this view (Supplemental Figs. 3 and 4). Albeit suggestive, this observation may not be conclusive and further experiments with a different strategy may be required to confirm the hypothesis.

Practical Implications. The majority of evidence available to date, mostly from studies in transgenic animals, identifies recovery of SR Ca^{2+} uptake function as a promising therapeutic strategy in heart failure (Schmidt et al., 2001; Haghighi et al., 2004); however, adverse effects have also been reported (Chen et al., 2004; Vangheluwe et al., 2006). The net outcome of this approach probably depends on the extent of SR uptake enhancement, which may be difficult to adjust if gene therapy is used. Under this aspect, availability of pharmacological tools for modulation of SR function would be highly desirable; however, it is unclear whether deranged SR function can be recovered by pharmacological means. Previous studies in animal models (Mattera et al., 2007; Micheletti et al., 2007; Sabbah et al., 2007) and man (Ghali et al., 2007) showed that the positive inotropic effect of istaroxime is retained in the failing myocardium, but it was unknown whether stimulation of SR Ca^{2+} uptake could still contribute to it. The present results not only prove that this is the case but show that almost complete recovery of failing SR uptake function might be achieved by pharmacological means. In addition to contractility, SR function may also affect myocardial electrical stability. Istaroxime is also a Na^+/K^+ pump inhibitor, but it is definitely less proarrhyth-

mic than digoxin in animal studies (Micheletti et al., 2002; Rocchetti et al., 2003), and preliminary clinical evidence corroborates this finding (Ferrari et al., 2007; Ghali et al., 2007). The electrophysiological actions of the two substances have been thoroughly compared (Rocchetti et al., 2003), and the only mechanism found to account for the different arrhythmogenicity is stimulation of SR Ca^{2+} uptake (Rocchetti et al., 2005). This suggests that contractile recovery is not the only goal that may be achieved by modulation of SR function. The mechanism by which SR stimulation by istaroxime improves electrical stability is currently under evaluation.

Study Limitations. In the specific hypertrophy model used by this study, decreased SERCA2 activity occurs in the presence of normal SERCA2 protein expression (Micheletti et al., 2007), and this may represent a prerequisite for functional recovery by pharmacological means. This might prevent full extrapolation of the present findings to conditions in which SERCA2 expression is reduced. Nevertheless, a decrease in the ratio between SERCA2 and (unphosphorylated) PLB is a general feature of the failing myocardium (Haghighi et al., 2004), thus suggesting that functional down-regulation may have a general role in SR dysfunction. Thus, significant, even if incomplete, recovery might theoretically be achieved by pharmacological means in most cases.

Acknowledgments

We thank Giuseppe Bianchi for providing constructive discussion throughout the execution of the study, Bruno Gavillet for reviewing the manuscript, Fiorentina Palazzo and Barbara Moro for guinea pig aortic banding, and Mara Ferrandi for Western blot experiments (Supplemental Fig. 3).

References

Ahmmed GU, Dong PH, Song G, Ball NA, Xu Y, Walsh RA, and Chiamvimonvat N (2000) Changes in $Ca^{(2+)}$ cycling proteins underlie cardiac action potential prolongation in a pressure-overloaded guinea pig model with cardiac hypertrophy and failure. *Circ Res* **86:**558–570.

Barcenas-Ruiz L, Beuckelmann DJ, and Wier WG (1987) Sodium-calcium exchange in heart: membrane currents and changes in $[Ca^{2+}]_i$. *Science* **238:**1720–1722.

Bers DM (2002a) Ca sources and sinks, in *Excitation-Contraction Coupling and Cardiac Contractile Force* (Bers DM ed) pp 39–62, Kluwer Academic Publishers, Boston, MA.

Bers DM (2002b) Excitation-contraction coupling, in *Excitation-Contraction Coupling and Cardiac Contractile Force* (Bers DM ed) pp 203–244, Kluwer Academic Publishers, Boston, MA.

Bers DM (2002c) Sarcolemmal Na/Ca exchange and Ca-pump, in *Excitation-Contraction Coupling and Cardiac Contractile Force* (Bers DM ed) pp 133–160, Kluwer Academic Publishers, Boston, MA.

Bers DM (2002d) Ultrastructure, in *Excitation-Contraction Coupling and Cardiac Contractile Force* (Bers DM ed) pp 1–18, Kluwer Academic Publishers, Boston, MA.

Bers DM (2006) Altered cardiac myocyte Ca regulation in heart failure. *Physiology* **21**:380–387.

Bers DM and Berlin JR (1995) Kinetics of $[Ca]_i$ decline in cardiac myocytes depend on peak $[Ca]_i$. *Am J Physiol Cell Physiol* **268:**C271–C277.

Chen Y, Escoubet B, Prunier F, Amour J, Simonides WS, Vivien B, Lenoir C, Heimburger M, Choqueux C, Gellen B, et al. (2004) Constitutive cardiac overexpression of sarcoplasmic/endoplasmic reticulum Ca^{2+}-ATPase delays myocardial failure after myocardial infarction in rats at a cost of increased acute arrhythmias. *Circulation* **109:**1898–1903.

Díaz ME, Graham HK, and Trafford AW (2004) Enhanced sarcolemmal Ca^{2+} efflux reduces sarcoplasmic reticulum Ca^{2+} content and systolic Ca^{2+} in cardiac hypertrophy. *Cardiovasc Res* **62:**538–547.

Ferrari P, Micheletti R, Valentini G, and Bianchi G (2007) Targeting SERCA2a as an innovative approach to the therapy of congestive heart failure. *Med Hypotheses* **68:**1120–1125.

Ghali JK, Smith WB, Torre-Amione G, Haynos W, Rayburn BK, Amato A, Zhang D, Cowart D, Valentini G, Carminati P, et al. (2007) A phase 1–2 dose-escalating study evaluating the safety and tolerability of istaroxime and specific effects on electrocardiographic and hemodynamic parameters in patients with chronic heart failure with reduced systolic function. *Am J Cardiol* **99**:47A–56A.

Grynkiewicz G, Poenie M, and Tsien RY (1985) A new generation of Ca^{2+} indicators with greatly improved fluorescence properties. *J Biol Chem* **260:**3440–3450.

Haghighi K, Gregory KN, and Kranias EG (2004) Sarcoplasmic reticulum ca-ATPase-phospholamban interactions and dilated cardiomyopathy. *Biochem Biophys Res Commun* **322:**1214–1222.

Institute of Laboratory Animal Resources (1996) *Guide for the Care and Use of Laboratory Animals*, 7th ed, Commission on Life Sciences, National Research Council, Washington DC.

Kawai M, Hussain M, and Orchard CH (1998) Cs^+ inhibits spontaneous Ca^{2+} release from sarcoplasmic reticulum of skinned cardiac myocytes. *Am J Physiol Heart Circ Physiol***275:**H422–H430.

Kiss E, Ball NA, Kranias EG, and Walsh RA (1995) Differential changes in cardiac phospholamban and sarcoplasmic reticular $Ca^{(2+)}$-ATPase protein levels: effects on Ca^{2+} transport and mechanics in compensated pressure-overload hypertrophy and congestive heart failure. *Circ Res* **77:**759–764.

Lee KS, Marban E, and Tsien RW (1985) Inactivation of calcium channels in mammalian heart cells: joint dependence on membrane potential and intracellular calcium. *J Physiol* **364:**395–411.

Mattera GG, Lo GP, Loi FM, Vanoli E, Gagnol JP, Borsini F, and Carminati P (2007) Istaroxime: a new luso-inotropic agent for heart failure. *Am J Cardiol* 99:33A–40A.

Meissner G and Henderson JS (1987) Rapid calcium release from cardiac sarcoplasmic reticulum vesicles is dependent on Ca^{2+} and is modulated by Mg^{2+}, adenine nucleotide, and calmodulin. *J Biol Chem* **262:**3065–3073.

Micheletti R, Mattera GG, Rocchetti M, Schiavone A, Loi MF, Zaza A, Gagnol RJ, De Munari S, Melloni P, Carminati P, et al. (2002) Pharmacological profile of the novel inotropic agent (*E,Z*)-3-((2- aminoethoxy)imino)androstane-6,17-dione hydrochloride (PST2744). *J Pharmacol Exp Ther* **303:**592–600.

Micheletti R, Palazzo F, Barassi P, Giacalone G, Ferrandi M, Schiavone A, Moro B, Parodi O, Ferrari P, and Bianchi G (2007) Istaroxime, a stimulator of sarcoplasmic reticulum calcium adenosine triphosphatase isoform 2a activity, as a novel therapeutic approach to heart failure. *Am J Cardiol* **99:**24A–32A.

Pieske B, Maier LS, Bers DM, and Hasenfuss G (1999) Ca^{2+} handling and sarcoplasmic reticulum Ca^{2+} content in isolated failing and nonfailing human myocardium. *Circ Res* **85:**38–46.

Rocchetti M, Besana A, Mostacciuolo G, Ferrari P, Micheletti R, and Zaza A (2003) Diverse toxicity associated with cardiac Na^+/K^+ pump inhibition: evaluation of electrophysiological mechanisms. *J Pharmacol Exp Ther* **305:**765–771.

Rocchetti M, Besana A, Mostacciuolo G, Micheletti R, Ferrari P, Sarkozi S, Szegedi C, Jona I, and Zaza A (2005) Modulation of sarcoplasmic reticulum function by Na^+/K^+ pump inhibitors with different toxicity: digoxin and PST2744 [(*E,Z*)-3-((2-aminoethoxy)imino)androstane-6,17-dione hydrochloride]. *J Pharmacol Exp Ther* **313:**207–215.

Sabbah HN, Imai M, Cowart D, Amato A, Carminati P, and Gheorghiade M (2007) Hemodynamic properties of a new-generation positive luso-inotropic agent for the acute treatment of advanced heart failure. *Am J Cardiol* **99:**41A–46A.

Schmidt AG, Edes I, and Kranias EG (2001) Phospholamban: a promising therapeutic target in heart failure? *Cardiovasc Drugs Ther* **15:**387–396.

Shannon TR, Ginsburg KS, and Bers DM (2000) Reverse mode of the sarcoplasmic reticulum calcium pump and load- dependent cytosolic calcium decline in voltage-clamped cardiac ventricular myocytes. *Biophys J* **78:**322–333.

Sipido KR and Callewaert G (1995) How to measure intracellular $[Ca^{2+}]$ in single cardiac cells with fura-2 or indo-1. *Cardiovasc Res* **29:**717–726.

Studer R, Reinecke H, Bilger J, Eschenhagen T, Böhm M, Hasenfuss G, Just H, Holtz J, and Drexler H (1994) Gene expression of the cardiac Na^+ and Ca^{2+} exchanger in end stage human heart failure. *Circ Res* **75:**443–453.

Vangheluwe P, Tjwa M, Van Den BA, Louch WE, Beullens M, Dode L, Carmeliet P, Kranias E, Herijgers P, Sipido KR, et al. (2006) A SERCA2 pump with an increased Ca^{2+} affinity can lead to severe cardiac hypertrophy, stress intolerance and reduced life span. *J Mol Cell Cardiol* **41:**308–317.

Waggoner JR, Huffman J, Froehlich JP, and Mahaney JE (2007) Phospholamban inhibits Ca-ATPase conformational changes involving the E2 intermediate. *Biochemistry* **46:**1999–2009.

Weber CR, Ginsburg KS, Philipson KD, Shannon TR, and Bers DM (2001) Allosteric regulation of Na/Ca exchange current by cytosolic Ca in intact cardiac myocytes. *J Gen Physiol* **117:**119–131.

Xu L and Meissner G (1998) Regulation of cardiac muscle Ca^{2+} release channel by sarcoplasmic reticulum lumenal Ca^{2+}. *Biophys J* **75:**2302–2312.

Yano M, Ikeda Y, and Matsuzaki M (2005) Altered intracellular Ca^{2+} handling in heart failure. *J Clin Invest* **115:**556–564.

Zaza A, Rocchetti M, Brioschi A, Cantadori A, and Ferroni A (1998) Dynamic Ca^{2+}-induced inward rectification of K^+ current during the ventricular action potential. *Circ Res* **82:**947–956.

Zicha S, Moss I, Allen B, Varro A, Papp J, Dumaine R, Antzelevitch C, and Nattel S (2003) Molecular basis of species-specific expression of repolarizing K^+ currents in the heart. *Am J Physiol Heart Circ Physiol* **285:**H1641–H1649.

Address correspondence to: Dr. Antonio Zaza, Dipartimento di Biotecnologie e Bioscienze, Università degli Studi Milano-Bicocca, P.zza della Scienza 2, 20126 Milano, Italy. E-mail: antonio.zaza@unimib.it